JOURNAL OF MATERIALS SCIENCE 32 (1997) 6519–6523

Environmental assisted fracture for 4340 steel in water and air of various humidities

A. OEHLERT, A. ATRENS
Department of Mining, Minerals and Materials Engineering, The University of Queensland, Brisbane Qld 4072, Australia

This paper reports on measurements of crack growth by environmental assisted fracture (EAF) for 4340 steel in water and in air at various relative humidities. Of most interest is the observation of slow crack propagation in dry air. Fractographic analysis leads to the strong suggestion that this slow crack propagation is due to hydrogen cracking caused by internal hydrogen in solid solution inside the sample material.

1. Introduction

Environmental assisted fracture (EAF) [1] is an ongoing concern for high strength steels in which the susceptibility to EAF in water increases very significantly with increasing strength level [2, 3]. EAF is a complex multi-step process [1] in which crack advance occurs by an interaction of the applied loading, the plastic response of the material at the crack tip, the interaction of crack tip plasticity and surface passive protective films, and localized corrosion in the crack tip region in a local solution which can be very different to that of the bulk. Crack tip corrosion can liberate hydrogen which can be involved in the crack advance mechanism by hydrogen embrittlement (HE). When EAF is caused by hydrogen, the hydrogen source can be internal as hydrogen dissolved in solid solution in the metal.

EAF [1] often occurs under corrosive conditions where general corrosion is not a problem. The corrosion resistance of interest is caused by surface films that separate the material from its environment. Such films can cause a low rate of general corrosion despite a large thermodynamic driving force for corrosion. For example, stainless steels are stainless because of a very thin passive surface layer which is essentially Cr_2O_3. Although this layer is so thin (typically less than 4 nm [4–7]) that it cannot be seen with the naked eye, this layer is nevertheless effective in separating the steel from its environment. The passive films on stainless steels are usually self repairing. The breakdown of such films can be induced chemically (e.g. by chlorides), and pitting corrosion results when the breakdown is localized. Localized film breakdown under the joint action of a stress and an environment is the essence of EAF. Cracking of surface films has been shown to be involved for EAF initiation in pipeline steels [8, 9] and high strength steels [10–12].

Our prior work has dealt extensively with the EAF of steels. A new test method for EAF was developed [13, 14]: the linearly increasing stress test (LIST) was applied to high strength steels [13, 14], pipeline steels [8], carbon steel [15] and pure copper [16]. Stress rate effects have been shown [8–16] to be an important part of the EAF mechanism, and, in particular, crack tip creep has been shown to be an important part of the EAF mechanism for high strength steels undergoing EAF in water [8–17], which can provide [17] an explanation for the stationary cracks observed in service. Room temperature creep has been measured for high strength steels including AISI 4340 and AerMet100 [18] and related to crack initiation [11]. A new model was proposed for stress corrosion cracking (SSC) for quenched and tempered steels based on strain-assisted dissolution [19]. Stress corrosion crack velocity was measured [20] and was related to heat treatment and microstructure [21, 22]. The possible causes for the intergranular crack path for high strength steels undergoing EAF in water have been explored by microstructural characterization using electron microscopy [23–25], measurements of grain boundary chemistry [26] and electrochemistry [27]. A precipitation strengthened duplex stainless steel was developed [28].

This paper reports on measurements of the EAF of a steel (4340) in water and in air at various relative humidities. Of most interest is the observation of slow crack propagation in dry air. Fractographic analysis leads to the strong suggestion that this slow crack propagation is due to hydrogen cracking caused by internal hydrogen in solid solution inside the sample material.

2. Experimental procedure

The EAF crack propagation measurements were carried out using fatigue precracked double cantilever beam specimens ($10 \times 60 \times 100$ mm) stressed under conditions of constant load or constant displacement to a desired initial stress intensity at the crack tip. Various applied stress intensities were used in the range 20 to 40 MPa $m^{1/2}$. These were all well above K_{1SCC} for as-quenched 4340 in water, which is in the range 10–15 MPa $m^{1/2}$. The constant displacement rig was instrumented as described previously [20] so

0022–2461

that load and crack opening displacement (COD) measurements could be continuously recorded; calibration allowed continuous measurement of crack velocity while the specimen was exposed to the environment of interest. The chemical composition of the 4340 is given in Table I and the mechanical properties are given in Table II. The double cantilever beam specimens were machined to final dimensions before heat treatment: 5 h at 870 °C, oil quenched. After heat treatment a 35 mm long slot was cut down the centreline with a cutoff wheel and the fatigue precracking was carried out. All experiments were carried out at 21°C. Scanning electron microscopy was used to examine fracture surface after testing.

3. EAF velocity measurements

The EAF crack velocity was measured for as-quenched 4340 in distilled water and in laboratory air of 80% RH at applied stress intensities of 20 and 30 MPa $m^{1/2}$ in both the constant displacement (CD) and constant load (CL) test rigs, and the results are summarized in Table III. The EAF crack velocity was measured to be 3×10^{-4} m s^{-1}, in good agreement with our prior measurements [17].

Specimen D1 was tested in air dried only with silica gel. This specimen showed extensive crack growth soon after loading to 40 MPa $m^{1/2}$. No determination of crack velocity was made, although the short time involved indicated a high crack velocity. The present result was consistent with the prior observations [17] that the crack velocity of as-quenched 4340 in air dried only with silica gel was about an order of magnitude lower than the velocity in distilled water.

Specimen D2 was tested in air dried with a two stage drying column; the first column was filled with silica gel (SG) and the second column was filled with phosphorus pentoxide (PPO). This drying process should result in a water content in the air of less than 2.5×10^{-5} g l^{-1}. The recorded COD and load data indicated continuous crack growth with an average crack velocity of 8×10^{-9} m s^{-1} (Fig. 1).

Specimen D3 was dried in a furnace for 3 h at 105 °C immediately before introduction into the dry air of the environmental cell, which was dried with the two-stage drying column as for the test with specimen D2. Furthermore, approximately 100 g phosphorus pentoxide was also placed inside the environmental cell. There was slow crack growth at 9×10^{-9} m s^{-1}.

Specimens D4 and D5 were furnace dried for 3 h at 105 °C immediately before introduction into the dry air of the environmental cell with approximately 100 g phosphorous pentoxide as for the test with specimen D3. They remained in the dry air for 10 h before loading to 40 MPa $m^{1/2}$. After 24 h they were unloaded, removed from cell, and broken open after the crack had been extended by fatigue. Both specimens exhibited slow crack growth in the dry air environment with an average crack velocity of 4×10^{-9} m s^{-1}.

TABLE I Chemical composition (wt %)

C	Cr	Ni	Mn	Mo	P	S	Si	V
0.36	1.64	1.5	0.6	0.25	0.01	0.005	0.30	0.06

TABLE II Mechanical properties

Hardness (HRC)	$\sigma_{0.01\%}$ (MPa)	$\sigma_{0.2\%}$ (MPa)	UTS (MPa)
58	810	1490	2100

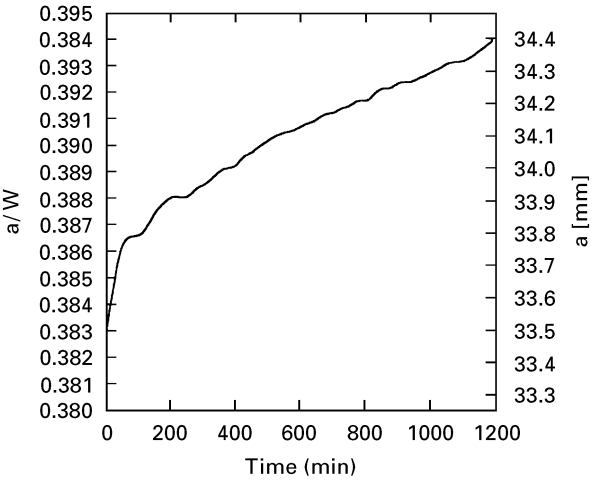

Figure 1 Crack length (*a*) as a function of test time for test D2: as-quenched 4340 loaded at 34 MPa $m^{1/2}$ in dry air at room temperature.

TABLE III Crack velocity measurements for as-quenched 4340 at 21°C

Test	Environment	K_{appl} (MPa $m^{1/2}$)	Rig type	Crack velocity (m s^{-1})
1	Distilled water	20	CL	3×10^{-4}
2	Distilled water	30	CD	3×10^{-4}
3	Laboratory air, 80% RH	20	CL	3×10^{-4}
4	Laboratory air, 80% RH	30	CD	3×10^{-4}
D1	Air dried with SG	40	CL	nm
D2	Air dried with SG + PPO	34	CD	8×10^{-9}
D3	3 h at 105 °C, air dried with SG + PPO	34	CD	9×10^{-9}
D4	3 h at 105 °C, air dried with SG + PPO	40	CD	4×10^{-9}
D5	3 h at 105 °C, air dried with SG + PPO	40	CD	4×10^{-9}

nm = not measured.

4. Fractography

The fracture morphology of the fatigue precracks exhibited areas which were predominantly intergranular (as illustrated in Fig. 2) as well as regions which were predominantly transgranular in appearance. There were very few areas with a mixed inter-/transgranular morphology. There were no distinct fatigue striations. In areas with a predominantly intergranular fatigue mode, it was sometimes difficult to distinguish between the end of the fatigue precrack and the start of EAF. However, there was a sharp transition between transgranular fatigue and EAF, as shown by Fig. 3.

EAF in distilled water was predominantly intergranular as shown in Fig. 4, as is typical for EAF of high strength steels in water. Note the large amount of markings on the grain facets and the voids which had developed on the grain walls which suggest that a significant amount of plasticity occurred locally despite the macroscopically brittle fracture.

The fracture morphology for EAF in air dried only with silica gel is shown in Figs 5 and 6 for specimen D1. The fracture was predominantly intergranular

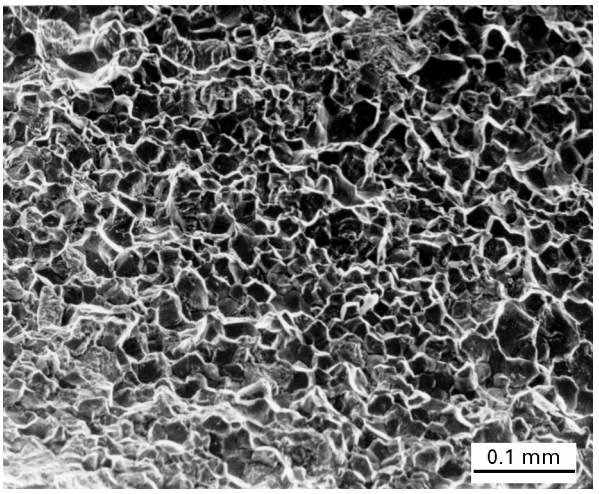

Figure 2 Predominantly intergranular fatigue in as-quenched 4340.

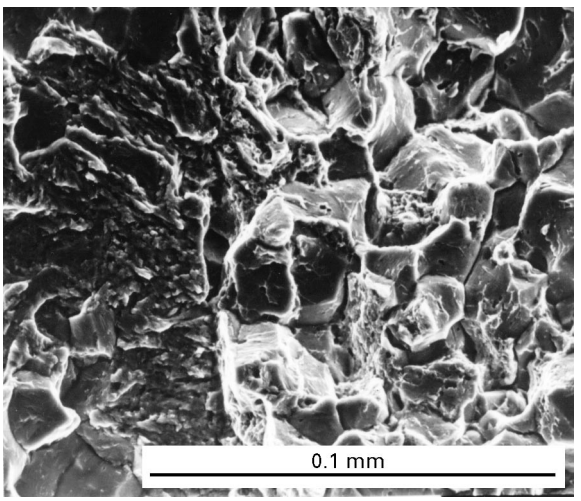

Figure 3 Transition between predominantly transgranular fatigue and predominantly intergranular EAF; EAF was for as-quenched 4340 in distilled water at 21°C.

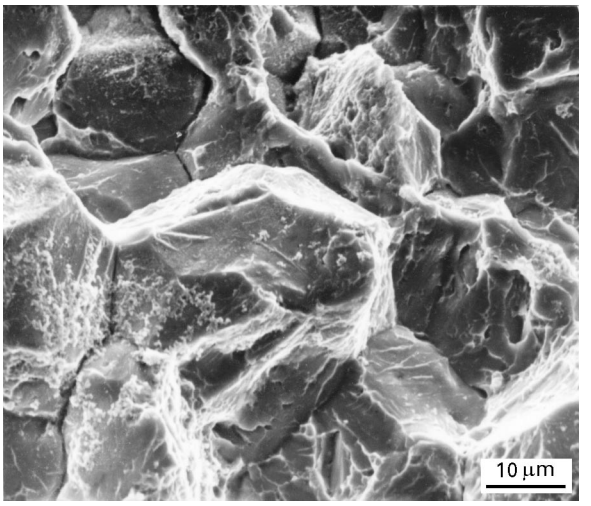

Figure 4 Predominantly intergranular EAF in as-quenched 4340 in distilled water at room temperature and 40 MPa $m^{1/2}$.

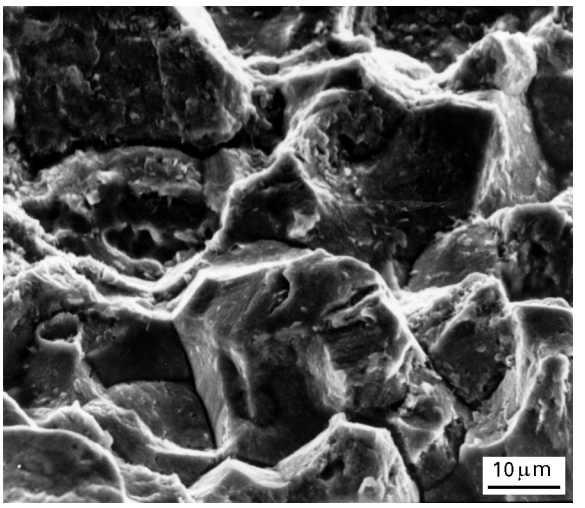

Figure 5 Predominantly intergranular EAF in specimen D1: as-quenched 4340 in air dried with silica gel at room temperature and 40 MPa $m^{1/2}$.

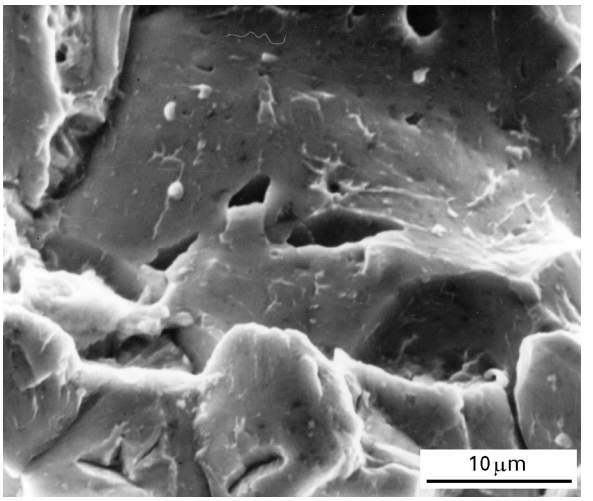

Figure 6 SEM micrograph showing voids on grain boundary facets for specimen D1: as-quenched 4340 in air dried with silica gel at room temperature and 40 MPa $m^{1/2}$.

with some areas of mixed inter-/transgranular mode. The grain facets exhibited less signs of ductility, except in a few areas where the grains were completely covered with dimples. However, there was an increased amount of voids on the grain walls, as illustrated in Fig. 6.

The fractography of EAF in dry air (i.e. dried with both silica gel and phosphorus pentoxide) for specimens D4 and D5 was examined in detail. EAF extended over the entire specimen width between the initial and final fatigue cracks and exhibited approximately equal amounts of two distinct fracture morphologies: intergranular fracture and dimple rupture. Fig. 7 shows the transition region between transgranular fatigue to a region which exhibits a large number of dimples followed by a predominantly intergranular fracture mode. Fig. 8 shows the transition between transgranular fatigue to dimple rupture, which is shown at higher magnification in Fig. 9. The dimple morphology varied from large and shallow to small and deep.

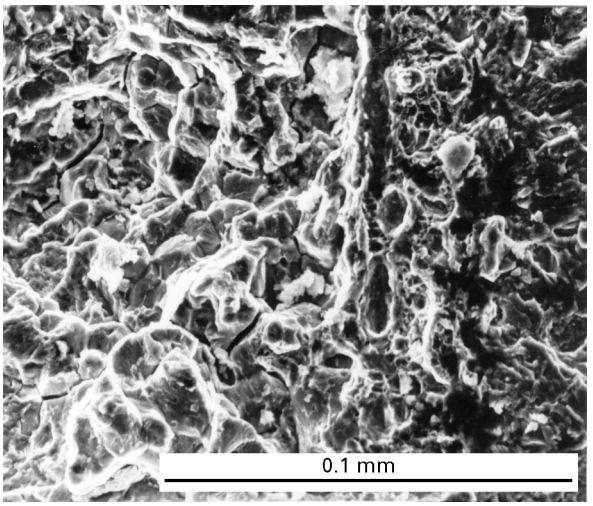

Figure 7 The transition region between transgranular fatigue to a region which exhibits a large number of dimples followed by a predominantly intergranular fracture mode. As-quenched 4340 in air dried with silica gel plus phosphorus pentoxide at room temperature and 40 MPa $m^{1/2}$.

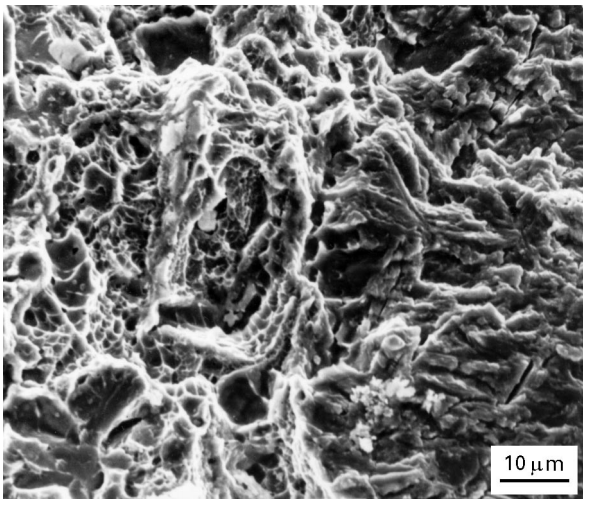

Figure 8 The transition between transgranular fatigue to EAF with a dimple rupture morphology: as-quenched 4340 in air dried with silica gel plus phosphorus pentoxide at room temperature and 40 MPa $m^{1/2}$.

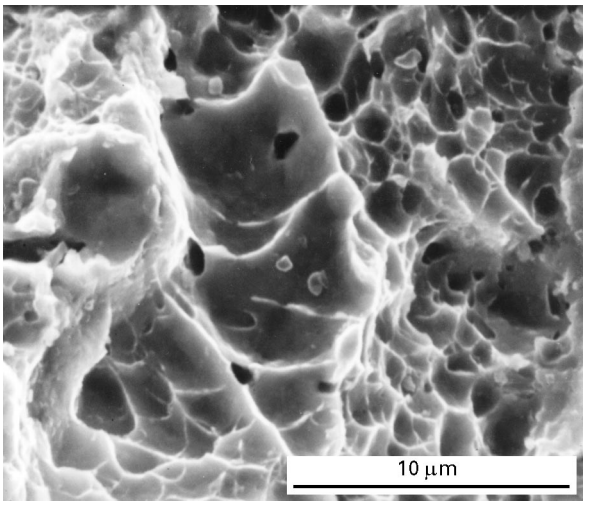

Figure 9 Higher magnification micrograph of Fig. 8.

5. Discussion

In the present study slow crack growth was observed in distilled water. The crack velocity and intergranular nature was in agreement with prior studies [17]. Slow crack growth in the present work in humid air (80% RH) and air dried with silica gel was also consistent with the prior work [17]. It is possible that capillary condensation occurs in the crack tip region even in the air dried with silica gel and that the condensed water provides the environment for EAF. The fractography in the present work indicated an intergranular fracture mode in the air dried with silica gel. This intergranular fracture mode was very similar to that observed for slow crack growth in water. This would be consistent with a similar propagation mechanism in both cases.

The most interesting specimens in the present study are those showing EAF in the air dried with both silica gel and phosphorus pentoxide (specimens D2 to D5). The initial experiment was unexpected as it was in contradiction to the prior work [17]. Because of this contradiction experiment D2 was repeated in experiments D3 and D4 with increasing care to exclude all sources of water, and experiment D4 was itself repeated in experiment D5. All these experiments D2 to D5 showed slow crack growth, and the crack velocity was similar in all cases. Thus there was no doubt that slow crack growth was occurring in this batch of as-quenched 4340 in dry air with a crack velocity about five orders of magnitude lower than the velocity for crack propagation in water or laboratory air of 80% RH.

The fractography for EAF in dry air exhibited approximately equal amounts of two distinct fracture morphologies: intergranular fracture and dimple rupture. This was quite different to the fractography for crack propagation in water or laboratory air of 80% RH, indicating that the EAF mechanism in dry air is different to that for EAF in water.

Fatigue propagation with a predominantly intergranular morphology has been reported previously

[29–32] and associated with internal hydrogen [32]. Cheruvu [32] found that 4340 specimens without internal hydrogen exhibited transgranular fatigue crack growth with less than 1% intergranular fatigue, independent of applied stress intensity amplitude and grain size. Cathodically charged specimens showed much more intergranular fracture and a strong dependence on grain size. A grain size of 20 μm produced 80–85% intergranular fatigue, whereas a ten times larger grain size produced 10–20% intergranular fatigue – a significantly smaller fraction. These observations [32] strongly suggested the presence of internal hydrogen in the samples of 4340 used in the present work.

The presence of internal hydrogen would explain the observed crack propagation in the dry air environments when there was no crack advance in similar testing by Rieck *et al.* [17]. Furthermore, the presence of hydrogen inside the specimen would explain the large fraction of dimple rupture in these dry air environments.

6. Conclusions

Fracture mechanics tests of 4340 in distilled water and air of various levels of dryness revealed the following:

1. The EAF crack velocity was 3×10^{-4} m s^{-1} for as-quenched 4340 in distilled water and in laboratory air of 80% RH at applied stress intensities of 20 and 30 MPa m$^{1/2}$. The fractography was intergranular with significant signs of ductility.

2. Slow crack growth was observed for as-quenched 4340 in air dried only with silica gel at 40 MPa m$^{1/2}$. The fractography was intergranular similar to that for EAF in water, suggesting a similar cracking mechanism.

3. Slow crack growth was observed for as-quenched 4340 at 40 MPa m$^{1/2}$ in dry air, dried with both silica gel and phosphorus pentoxide. The fractography exhibited approximately equal amounts of two distinct fracture morphologies: intergranular fracture and dimple rupture. This was quite different to the fractography for crack propagation in water suggesting a different EAF mechanism in dry air.

4. The presence of intergranular fatigue suggests the presence of internal hydrogen which could explain the observed slow crack growth in the dry air.

References

1. A. ATRENS and Z. F. WANG, *Mater. Forum* **19** (1995) 9.
2. M. O. SPEIDEL, in "*Corrosion in power generating equipment*" edited by M. O. Speidel and A. Atrens (Plenum, New York and London, 1984) p. 85.
3. R. MAGDOWSKI-PEDRAZZOLI and M. O. SPEIDEL, in "*Parkins Symposium on fundamental aspects of stress corrosion cracking*", edited by S. M. Bruemmer, E. I. Meletis, R. H. Jones, W. W. Gerberich, F. P. Ford and R. W. Staehle (TMS, Pennsylvania, 1992) p. 341.
4. S. JIN and A. ATRENS, *Appl. Phys. A* **42** (1987) 149.
5. *Idem., ibid.* **50** (1990) 287.
6. A. S. LIM and A. ATRENS, *ibid.* **53** (1992) 273.
7. *Idem., ibid.* **54** (1992) 500.
8. Z. F. WANG and A. ATRENS, *Metall. Mater. Trans.* **27A** (1996) 2686.
9. *Idem., Mater. Sci. Engng*, accepted for publication.
10. A. ATRENS, Z. F. WANG, N. KINAEV, D. R. COUSENS and J. Q. WANG, in Proceedings of 13 International Corrosion Congress, Melbourne (1996) paper 233.
11. A. OEHLERT and A. ATRENS, *Mater. Forum* **17** (1993) 415.
12. *Idem., Corrosion Sci.* **38** (1996) 1159.
13. A. ATRENS, C. C. BROSNAN, S. RAMAMURTHY, A. OEHLERT and I. O. SMITH, *Measurement Sci. Technol.* **4** (1993) 1281.
14. S. RAMAMURTHY and A. ATRENS, *Corrosion Sci.* **34** (1993) 1385.
15. A. ATRENS and A. OEHLERT, *J. Mater. Sci.*, submitted for publication.
16. J. SALMOND and A. ATRENS, *Scripta Metall. Mater.* **26** (1992) 1447.
17. R. M. RIECK, A. ATRENS and I. O. SMITH, *Met. Trans.* **20 A** (1989) 889.
18. A. OEHLERT and A. ATRENS, Overview No 114 *Acta Metall. Mater.* **42** (1994) 1493.
19. A. ATRENS, R. M. RIECK and I. O. SMITH, in "*ICF7 Advances in fracture research*", edited by K. Salama, K. Ravi-Chandar, D. M. R. Taplin and P. Rama Rao (Pergamon Press, Oxford, 1989) p. 1603.
20. A. OEHLERT and A. ATRENS, *J. Mater. Sci.*, submitted for publication.
21. R. M. RIECK, A. ATRENS and I. O. SMITH, *Mater. Forum* **13** (1989) 48.
22. *Idem., Ibid.* **13** (1989) 54.
23. J. D. GATES, A. ATRENS and I. O. SMITH, *Z. fur Werkstofftechnik* **18** (1987) 165.
24. *Idem., ibid.* **18** (1987) 179.
25. *Idem., ibid.* **18** (1987) 344.
26. J. SKOGSMO and A. ATRENS, *Acta Metall. Mater.* **42** (1994) 1139.
27. S. RAMAMURTHY, A. ATRENS, I. O. SMITH, *Mater. Sci. Forum* **44 & 45** (1989) 139.
28. A. ATRENS, R. COADE, J. ALLISON, H. KOHL, G. HOCHOERTLER and G. KRIST, *Mater. Forum* **17** (1993) 263.
29. R. J. COOK, P. E. IRVING, G. S. BOOTH and C. J. BEEVERS, *Eng. Fract. Mech.* **7** (1975) 69.
30. P. E. IRVING and A. KURZFELD, *Met. Sci.* **12** (1978) 495.
31. R. O. RITCHIE and J. F. KNOTT, *Acta Metall.* **21** (1973) 639.
32. N. S. CHERUVU, *ASTM ASTP 827* (1984).

Received 11 July 1996
and accepted 24 July 1997